REGULAR ARTICLE

Magnetotropicity of five-membered heterocyclic molecules

Stefano Pelloni · Paolo Lazzeretti

Abstract Ab initio methods have been employed to obtain models for the current density field induced in the electrons of pentatomic cyclic molecules C_4H_4X, with $X = CH_2$, NH, O, S, PH, and AsH, in the presence of a static, homogeneous magnetic field normal to the plane containing the four ring carbon atoms. These models are expected to provide simple and valid tools to assess the magnetotropism of these compounds and to interpret their magnetic response.

Keywords Magnetic aromaticity · Five-membered heterocycles · Magnetically-induced current density · Stagnation graph

1 Introduction

The ring current model (RCM) developed by Pople [1,2] and McWeeny [3], allowing for earlier proposals by Pauling [4], Lonsdale [5], and London [6–8], provides an explanation of the enhanced diamagnetism typical of aromatic compounds. In benzene, for instance, an external magnetic field at right angles to the molecular plane induces currents in the delocalized π electrons, which flow round a closed conjugating path. The Biot-Savart magnetic field generated by these currents enhances the out-of-plane component of the susceptibility tensor and decreases the magnitude of the out-of-plane component of the shielding tensor at

S. Pelloni · P. Lazzeretti (✉)
Dipartimento di Chimica dell'Università degli
Studi di Modena, Via Campi 183,
41100 Modena, Italy
e-mail: lazzeret@unimo.it
URL: http://www.theochem.chimfar.unimo.it

the ring protons. A series of review articles recently appeared provide extended bibliographical information on several aspects of the RCM [9–13].

The first ab initio visualisation of the current density field, reported in the early eighties for the cyclopropenyl cation $C_3H_3^+$ and for the benzene molecules [14–16], showed some inconsistencies of the historical description [4–8], e.g., the π ring currents are not superconductive, and their intensity is not uniform over a given circuit. Later on it was observed that they contain paramagnetic contributions causing an undulating motion, which can be described as a leap-frog effect [17].

London had guessed the solution to the problem of benzene in a magnetic field to be given by a very simple model wavefunction, i.e., a linear combination of six atomic 2p orbitals, but a minimal basis set is inherently incapable to yield a realistic representation of the π current flow. In particular, a paramagnetic contribution to the perpendicular component of magnetic susceptibility in planar ring systems such as benzene cannot be predicted by a minimal basis set [9,17]. In the words of Musher [18], the failure of the historical RCM can be ascribed to the "poor, arbitrary guess" made by London. In fact, group-theoretical arguments and ab initio calculations show that deviations from diamagnetic ring currents can be observed by assuming a larger, e.g., double-zeta, basis set of atomic 2p orbitals [17].

A revised model, removing some of the unphysical assumptions made by London [6–8] and intrinsic drawbacks flawing the historical RCM, but confirming many of its essential features, started being developed [19]. The ab initio picture of streamlines and modulus of the magnetic-field induced current density [14–16], and successive improved representations [9,20,21], show that benzene, the prototype of diatropic system, is endowed

with a weak "paramagnetic core". More generally, in the presence of a field perpendicular to the molecular plane, all planar monocyclic, neutral or charged, aromatics with the shape of a regular polygon with n sides, give rise to n diamagnetic vortices about the C–C bonds, and to a central paramagnetic vortex about the C_n symmetry axis. This paramagnetic vortex, required to exist by a very general theorem demonstrated by Gomes [22–24], was observed in planar C_nH_n systems, for $n = 3, 4, \ldots, 8$ [25], and in five-membered heterocyclic systems, e.g., arsole [26].

The fundamental importance of physically sound models for the current density field induced by magnetic perturbations can hardly be overemphasized. For instance, a reliable interpretation of magnetic shielding at the nuclei of aromatic hydrogen and carbon atoms is easily arrived at via plots of the Biot-Savart shielding-density function, obtained by a simple one-to-one mapping of the current density field [27,28]. Significant conclusions are thus arrived at, e.g., the proton deshielding caused by π ring currents takes place in a quite small portion of the molecular domain about a C–H bond, whereas the distant part of a given circuit increases proton shielding [29–32]. It was similarly demonstrated that approximately 10% of the out-of-plane component of carbon shielding is due to the positive contributions of π ring currents flowing in the region of the other carbon atoms [33].

The present paper aims at determining simple and reliable models of the current density vector field for a few pentatomic mono-cyclic conjugated systems with general formula C_4H_4X, with $X = CH_2$, NH, O, S, PH, and AsH, which have stimulated a lively debate about magnetotropism [26,34–36] as a criterion to assess aromaticity [37–39]. These models are expected to provide useful information for understanding magnetic response of pentatomics.

A theoretical tool referred to as stagnation graph is described in Sect. 2. Section 3 reports the results obtained, i.e., three-dimensional models of the vector field and maps of electron current density which are interpreted allowing for them.

2 Three-dimensional current models via stagnation graphs

Clear-cut information on the essentials of the quantum-mechanical current density induced in the electrons of a molecule by an external magnetic field (which will be assumed spatially uniform and time-independent) is provided by a "stagnation graph" [22–24] (SG) that shows the isolated points and the manifolds at which

the current density vanishes, customarily referred to as "*singularities*".

These graphs yield an abridged and compact topological description of the current density vector field and help interpret molecular magnetic response, e.g., magnetic susceptibility and nuclear magnetic shielding. Moreover, they illustrate the spatial aspects of the electron flow and provide essential information of what is going on in the whole molecular domain, which is generally overlooked in most papers discussing ring currents. Usually, plots of current density are given only for certain reference planes, say that of the molecule, or that of nearly maximum π charge density, which is not sufficient to understand major physical features.

Certain statements commonly made, e.g., that a probe nucleus above ring currents experiences additional shielding, may be misleading and cause serious misunderstanding, unless the position of that nucleus in the current density field is specified to a good approximation. Magnetic shielding is mainly determined by the local electron flow and depends on the second inverse power of the distance of π currents. In fact, the stagnation graphs of planar monocyclic aromatics show that a nucleus at a distance greater than ≈ 2.5 bohr is immersed in the local diamagnetic circulation referred to as the *primary diamagnetic vortex* of the molecule, which mainly accounts for magnetic shielding [25].

The present study relies on the theoretical background briefly outlined in the following. More detailed presentations can be found elsewhere, see a review article [9] and references therein. The field $\mathbf{J}(\mathbf{r})$ in the proximity of a stagnation point $\mathbf{r}_0$ is described by a truncated power series,

$$J_\gamma(\mathbf{r}) = (r_\alpha - r_{0\alpha}) \left[\nabla_\alpha J_\gamma\right]_{\mathbf{r}=\mathbf{r}_0}$$
$$+ \frac{1}{2}(r_\alpha - r_{0\alpha})(r_\beta - r_{0\beta})\left[\nabla_\alpha \nabla_\beta J_\gamma\right]_{\mathbf{r}=\mathbf{r}_0} + \cdots \quad (1)$$

Customary tensor notation is employed, e.g., summation over repeated Greek indices is implied. Within the linear approximation, only the leading term in relationship (1) is retained, and the description of the field about a stagnation point reduces to an analysis of the Jacobian $\nabla_\alpha J_\gamma$, i.e., a 3×3 matrix with real coefficients, evaluated at the stagnation point $\mathbf{r}_0$.

The classification of stagnation points based on the (*rank, signature*) index [40], suggested in Refs. [22–24] is usually adopted [9,21,41]. The rank r is defined as the number of non-vanishing eigenvalues of the Jacobian, the signature s is the excess of positive over negative eigenvalues [42]. The continuity equation $\nabla_\alpha J_\alpha = 0$ for the stationary state constrains the Jacobian to be traceless all over the $\mathbf{J}$ field, so that only two eigenvalues are
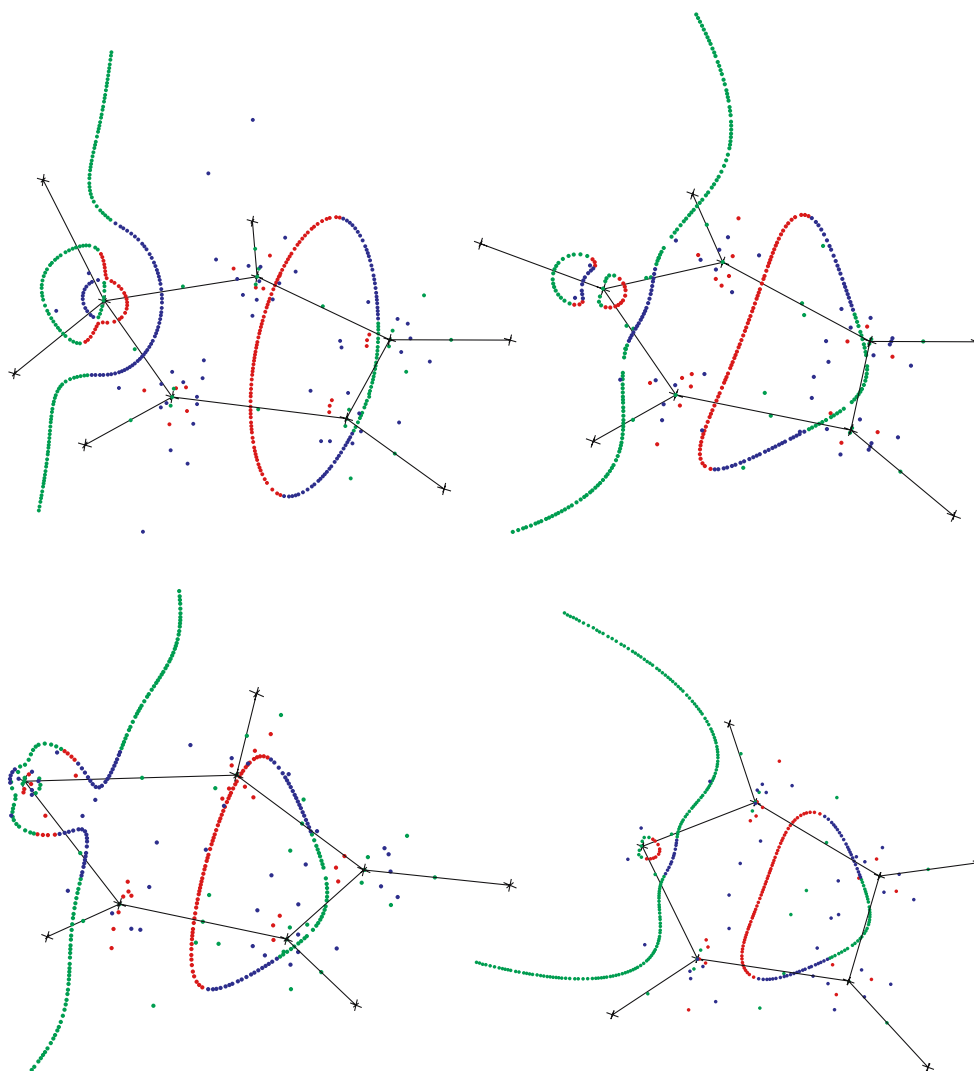
Fig. 1 The stagnation graph of five-membered cyclic compounds. Clockwise from *top left*: 1,3-cyclopentadiene, pyrrole, furan, and thiophene in the presence of a magnetic field perpendicular to the molecular plane. In all the figures, diamagnetic (paramagnetic) *vortices* are represented by *green (red)* lines, and *saddle* lines are *blue*. The stagnation lines lie entirely on the $R\sigma_v$ plane of magnetic symmetry. Complete graphs for all figures are available on the web at [58]

linearly independent. This means that only a few (r, s) are allowed [22–24,43]:

- $(3,\pm 1)$ points for isolated singularities. The eigenvalues satisfy the condition $\xi_3 = -\Re(\xi_1 + \xi_2)$. If ξ_1 and ξ_2 are real (they may also be $\xi_1 = \xi_2$), then a false *node* or a false *saddle* point (see Ref. [44] for the nomenclature) are observed in the plane of the eigenvectors $\mathbf{t}_1$ and $\mathbf{t}_2$ corresponding to ξ_1 and ξ_2. If ξ_1 and ξ_2 are complex conjugate, a *focus* is found.
- $(2,0)$ points; eigenvalues $\xi_3 = 0, \xi_1 = -\xi_2$. For real $\xi_{1,2} = \pm a$ (pure imaginary $\xi_{1,2} = \pm ib$), the phase portrait of a saddle (vortex) is found in the plane of the corresponding eigenvectors. Saddle- and vortex-

stagnation lines are continuous manifolds of $(2,0)$ points. In most cases they are symmetry determined and lie on molecular symmetry planes. $(2,0)$ points can be open lines (this is the case of *axial vortices*) or form close loops: a *toroidal* vortex flows up through the center and down around the sides of a closed vortex line of $(2,0)$ points [45]. Other closed loops formed by sequences of vortex- and saddle-lines separated by $(0,0)$ points, defined in the following, have been observed in diatropic planar ring molecules [25]. Diamagnetic (paramagnetic) axial vortices of the electronic current density rotate clockwise (anticlockwise) with respect to an observer placed at the North pole of the **B** field, depending on the local *vorticity*, i.e., the curl $\nabla \times \mathbf{J}(\mathbf{r}_0)$.
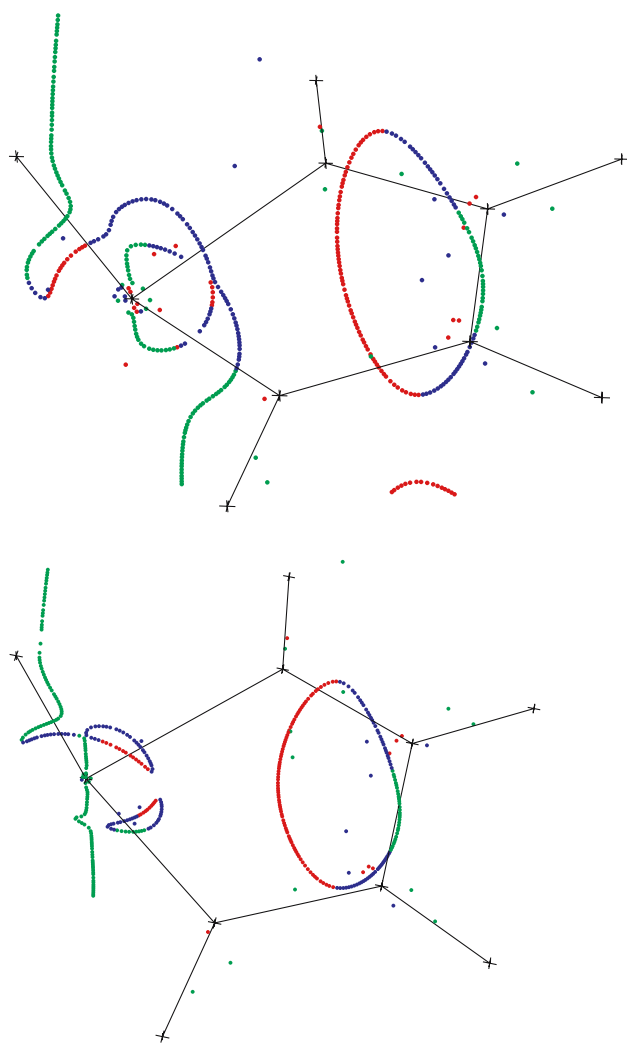
Fig. 2 The stagnation graph of five-membered heterocyclic compounds phosphole (above) and arsole in the presence of a magnetic field perpendicular to the plane containing the four carbon atoms. The stagnation lines lie entirely on the $R\sigma$ plane of magnetic symmetry
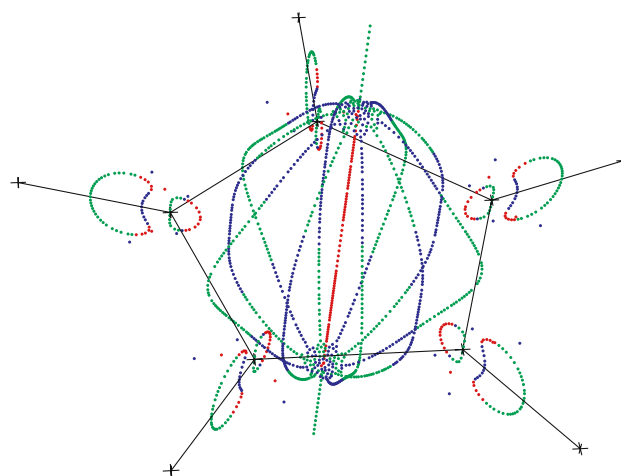

Fig. 3 The stagnation graph of the cyclopentadienyl anion $C_5H_5^-$ in a magnetic field normal to the molecular plane

For instance, the primary vortex line of the current density field induced by a magnetic field normal to the molecular plane of the cyclopentadienyl anion splits giving rise to six new vortex lines and five saddle lines, see Fig. 3. This branching conserves the total index $i_0 = +1$ of the primary vortex line.

The essential characteristics of the **J**-field can be guessed a priori in many cases, using rules dictated by magnetic group symmetry [9]. 1,3-Cyclopentadiene, furan, pyrrole, and thiophene in the presence of a magnetic field **B** perpendicular to the molecular plane are systems characterized by $\underline{2mm}$ symmetry in the International notation [46], i.e., $\overline{C_{2v}}(C_s) \equiv \{E\ RC_2\ R\sigma_v\ \sigma_v'\}$ in the Schönflies notation, with R the time-reversal operator. Phosphole and arsole in a magnetic field parallel to the σ symmetry plane belong to the $\underline{m}$ point group, i.e., $C_s(E) \equiv \{E\ R\sigma\}$. The diatropic cyclopentadienyl anion $C_5H_5^-$ has magnetic symmetry [25]

$$D_{5h}(C_{5h}) \equiv \left\{ E\ C_5\ C_5^2\ C_5^3\ C_5^4\ 5RC_2\ \sigma_h\ S_5\ S_5^7\ S_5^3\ S_5^9\ 5R\sigma_v \right\}.$$

A few relevant situations for pentatomic cyclic molecules with $C_{2v}(C_s)$ or $C_s(E)$ symmetry are the following:

- The σ_v' molecular plane cannot be crossed by trajectories of current density induced by a magnetic field at right angles to it.
- An $R\sigma_v$ (or $R\sigma$) plane can be crossed only by streamlines at right angles to it. If a streamline approaches such a plane forming an angle different from $\pi/2$, it is scattered, and the phase portrait of a saddle is observed. Therefore any (open or closed, vortex or saddle) stagnation line may lie on, but not pass
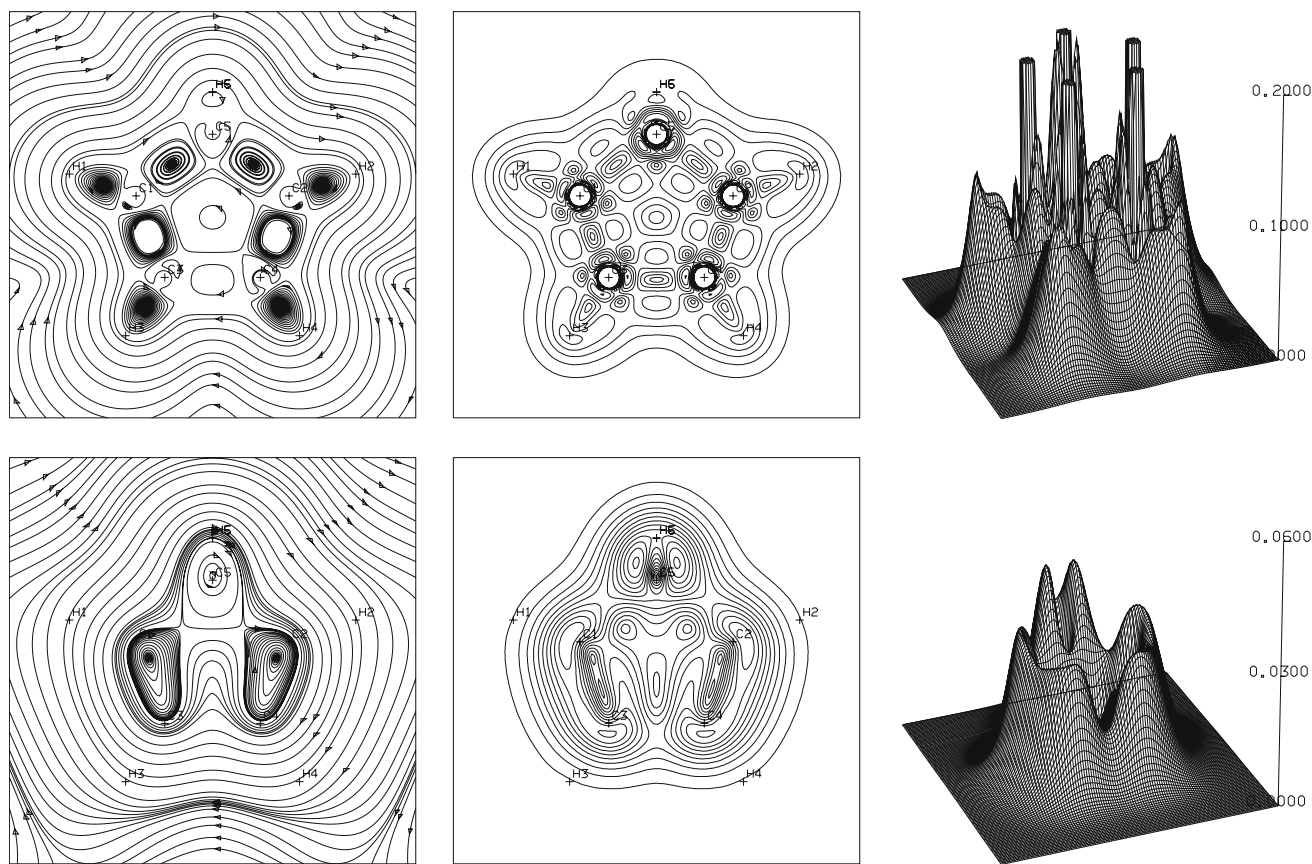
- (0,0) (*degenerate*) points corresponding to three zero eigenvalues of the Jacobian. They are also denoted as *transition points* at which branching of stagnation lines may occur.

The splitting of a stagnation line into several stagnation lines obeys the Gomes theorem [22–24,43]. Let us assume that the index of a saddle (vortex) line is -1 $(+1)$. When a stagnation line of index i_0 splits into m new lines, the sum of the indices of the stagnation lines coming out from the branching point is

$$\sum_{k=1}^{m} i_k = i_0. \tag{2}$$

Fig. 4 1,3-Cyclopentadiene molecule. *Top* streamlines, contour map (in steps of 2×10^{-2} au up to the maximum value 1.99 au) and three-dimensional perspective view of the modulus $|\mathbf{J}|$ (in au) for the total induced current density on the molecular plane. Here and in the following figures values of intensity higher than 2×10^{-1} au have been cut. *Bottom* streamlines, contour map (in steps of 3×10^{-3} au up to the maximum value ≈ 0.04 au) and three-dimensional perspective view of the π current density on a plane perpendicular to the inducing magnetic field, at 1.0 bohr above that of the molecule. The magnetic field (of magnitude 1 au) points outward, and diamagnetic circulation is clockwise

through, an $R\sigma$ plane, and cross perpendicularly, but not lie on, a σ'_v plane.

3 The stagnation graphs of planar cyclic pentatomics

We obtained spatial models for the current density induced in conjugated pentatomics of C_{2v} symmetry, C_4H_4X with $X = CH_2$, NH, O, and S, in a magnetic field perpendicular to the molecular plane, and in non planar homologs of C_s symmetry, C_4H_4PH and C_4H_4AsH, in a field perpendicular to the plane containing the four C atoms.

All the calculations have been carried out at the Hartree-Fock level of accuracy using extended basis sets, e.g., the uncontracted (13s10p5d2f/8s4p1d) for C/H in $C_5H_5^-$ from Ref. [25]. For C_5H_4X with $X = CH_2$, NH, O, S, PH, and AsH, the (13s8p/8s) basis sets from van

Duijneveldt [47] have been used for C, N, and O. The s basis has been augmented by a diffuse function with exponent 0.0399, 0.063, 0.046 respectively for C, O and N. These basis sets have been contracted to [9s6p/6s]. Three d functions with exponents 2.1409, 0.64240, 0.23613, and three p functions with exponents 2.0731, 0.49099, 0.15182 have been added on C and H respectively. The exponents of the d polarisation functions are 3.775, 1.3, 0.444 for O, and 2.837, 0.968, 0.335 for N. The S basis was taken from Ref. [48]. The (12s9p) P basis from Ref. [49] had been augmented with six d functions with exponents 14.4, 4.8, 1.6, 0.4, 0.133, and 0.0433. The uncontracted (21s14p10d2f) basis from Ref. [50] was used for As. Molecular geometries have been optimised at the B3LYP/6-31++G** level using the GAUSSIAN98 code [51].

The stagnation graph of five-membered cyclic molecules has been obtained by the approach of
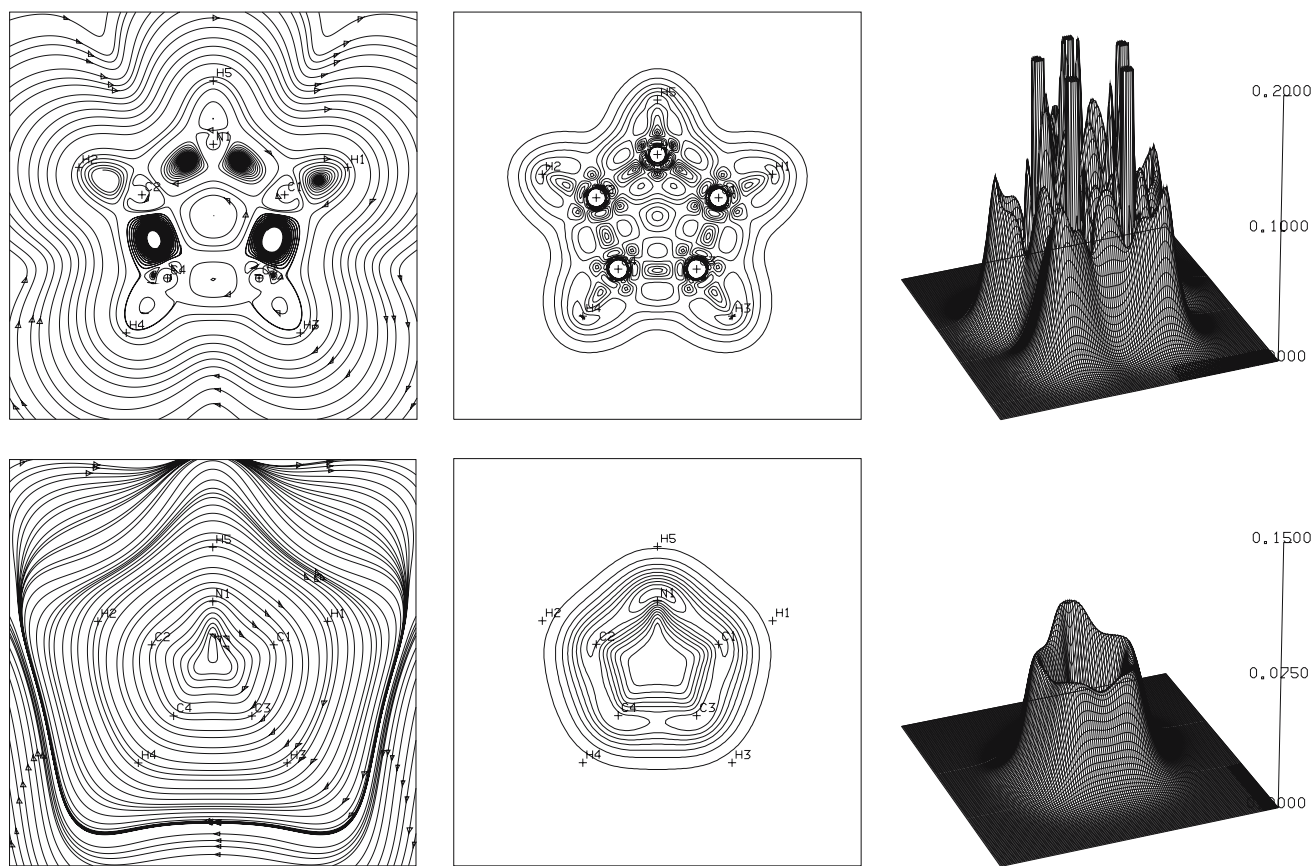
Fig. 5 Pyrrole molecule. *Top* streamlines, contour map (in steps of 2×10^{-2} au up to the maximum value 2.59 au) and three-dimensional perspective view of the modulus |**J**| (in au) for the total induced current density on the molecular plane. *Bottom* streamlines, contour map (in steps of 8×10^{-3} au up to the maximum value ≈ 0.08 au) and three-dimensional perspective view of the π current density on the plane perpendicular to the inducing magnetic field, at 1.0 bohr above that of the molecule. The magnetic field (of magnitude 1 au) points outward

continuous transformation of origin of the current density-diamagnetic zero (CTOCD-DZ) [9,20,52–54], allowing for the damped DZ2 formulation [55]. The current density evaluated via the CTOCD-DZ and DZ2 procedures is invariant to a change of coordinate system also in the case of approximate calculations [56], therefore these SGs would appear the same for any coordinate system.

Runge–Kutta procedures [57] were employed to obtain the streamline field by integrating the linear autonomous system of differential equations for the flow. The computational method has been outlined in a previous paper reporting the stagnation graph of six cyclic, planar aromatic molecules with $D_{nh}(C_{nh})$ magnetic symmetry [25].

The stagnation graphs of 1,3-cyclopentadiene, furan, pyrrole, and thiophene, in the presence of a magnetic field perpendicular to the molecular plane, are shown in Fig. 1, those for phosphole and arsole, in a magnetic field perpendicular to the plane through the ring carbon atoms, are shown in Fig. 2. However, as the graphs

are quite complicated topological objects, it is expedient to use a graphic software developed in our laboratory to obtain 3-dimensional representations that can be magnified and rotated by three Euler angles to analyse particular items in space [25,58].

There is striking difference between the graphs in Figs. 1 and 2 and those reported for C_nH_n (charged or neutral) aromatic cyclic molecules [25], which are characterized by a typical pattern: the primary diamagnetic vortex flowing in the outer portion of the molecular domain splits up into n diamagnetic vortices in correspondence of two (0,0) branching points (at a distance of ≈ 2.5 bohr for C_6H_6 and $C_5H_5^-$ [25]) above and below the molecular plane, giving rise to n diamagnetic vortices that terminate in the region of the C–C bonds, see, for instance, the SG for $C_5H_5^-$ in Fig. 3.

Instead, a common distinctive feature is typical of all the five-membered cyclic molecules of $C_{2v}(C_s)$ and $C_s(E)$ symmetry examined here, and it marks the peculiarity of their magnetic response, i.e., the closed stagnation loop disconnected from the rest of the SG,
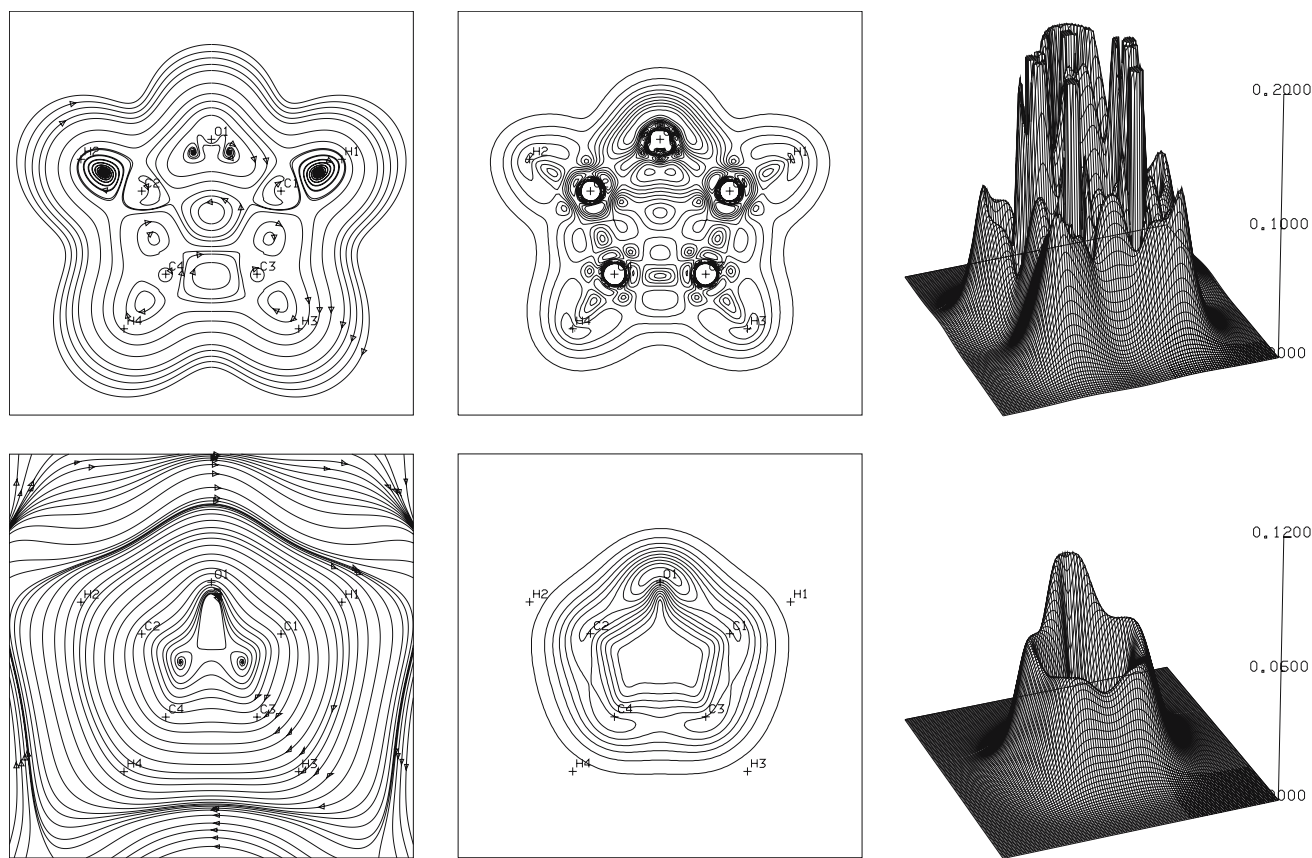
Fig. 6 Furan molecule. *Top* streamlines, contour map (in steps of 2×10^{-2} au up to the maximum value 4.39 au) and three-dimensional perspective view of the modulus |**J**| (in au) for the total induced current density on the molecular plane. *Bottom*: streamlines, contour map (in steps of 8×10^{-3} au up to the maximum value ≈0.08 au) and three-dimensional perspective of the π current density on the plane perpendicular to the inducing magnetic field, at 1.0 bohr above that of the molecule. The magnetic field (of magnitude 1 au) points outward

passing near-by the midpoint of the pentagon side opposite to the CH_2 moiety or the heteroatom. The (green) diamagnetic vortex line crossing the C-C bond and the (red) paramagnetic vortex line, flowing in the vicinity of the center of mass, are connected to (blue) saddle lines by (0,0) points, at which change of regime takes place. The Gomes index of this disconnected piece is 0, as two lines with opposite ±1 index emerge at each branching point.

A central paramagnetic vortex is expected to appear in all aromatic monocyclic molecules [9]. Its occurrence in pentatomic rings is documented by the red segment of the disconnected loop in the SGs of Figs. 1 and 2. On the other hand, the central paramagnetic vortex that constitutes the fingerprint of the aromatic systems with $D_{nh}(C_{nh})$ symmetry, whose presence is required by the Gomes theorem [22–24,43], is quite dissimilar to that in heterocyclic pentatomics.

In fact, the SGs show that the electron flow induced by a perpendicular magnetic field in pentatomic cyclic molecules with $C_{2v}(C_s)$ or $C_s(E)$ symmetry is characterized by a regime remarkably different from that of $D_{nh}(C_{nh})$ compounds. This feature must not be overlooked when aromaticity is discussed in terms of magnetic indicators, e.g., magnetic susceptibilities, nuclear magnetic shieldings, and central shielding, or nucleus-independent chemical shift [34,59].

The stagnation graphs of 1,3-cyclopentadiene, furan, pyrrole, and thiophene show another arrangement of common elements in the proximity of the CH_2 group or the heterotom, e.g., the (green) truncated vortex line, denoting diamagnetic flow which extends to the tail regions of the molecular domain. On crossing the plane of the nuclei, for the first three compounds, this stagnation line has a saddle character, and a small closed loop corresponding to two vortices flowing in opposite directions is observed in front of it in pyrrole and furan. More complicated patterns were found in the vicinity of the CH_2 moiety of 1,3-cyclopentadiene and near-by the sulphur atom in thiophene.
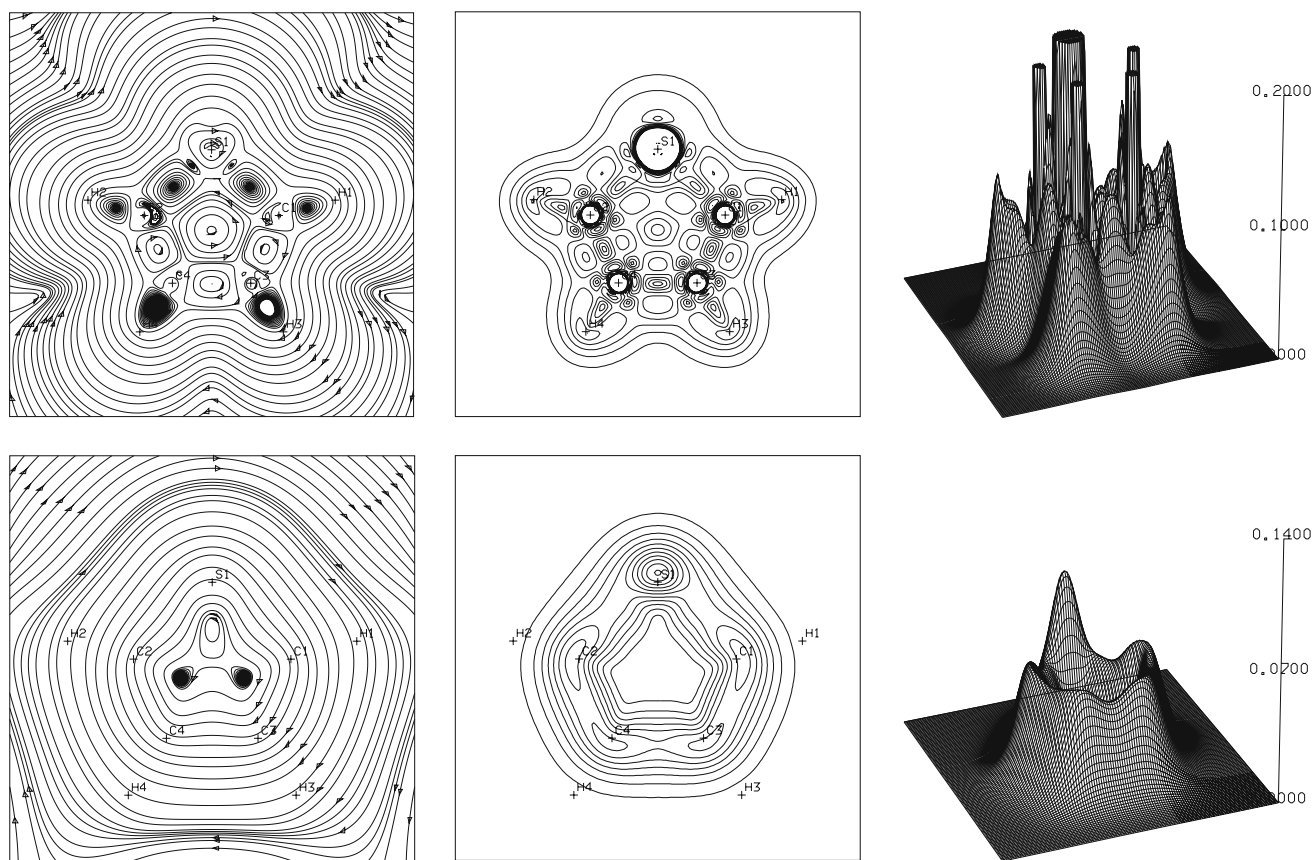
Fig. 7 Thiophene molecule. *Top* streamlines, contour map (in steps of 2×10^{-2} au up to the maximum value 8.14 au) and three-dimensional perspective view of the modulus |**J**| (in au) for the total induced current density on the molecular plane. *Bottom*: streamlines, contour map (in steps of 8×10^{-3} au up to the max-imum value $\approx$0.09 au) and three-dimensional perspective view of the π current density on a plane perpendicular to the inducing magnetic field, at 1.0 bohr above that of the molecule. The magnetic field (of magnitude 1 au) points outward

The "dust" of singular $(3, \pm 1)$ points observed in the graphs corresponds to local features of the vector field that are comparatively less interesting. However, they are useful for correct interpretation of the streamline plots in the current density field in the σ'_v molecular plane of 1,3-cyclopentadiene, furan, pyrrole, and thiophene, see Figs. 3, 4, 5, 6, 7.

Inspection of the SGs in Figs. 1 and 2 clearly shows that, on the one hand, there is only one axial vortex in C_5H_4X systems, passing through the C–C bond in front of the methylene group CH_2, or the heteroatom X=NH, O, S. On the other hand, electrons move in steady spiralling streams above and below the molecular plane (which cannot be crossed for magnetic symmetry reasons) in the region of the other bonds in the rings. Thus, the corresponding isolated singularities observed in the SGs are $(3, \pm 1)$ foci.

This regime reminds that observed in ethylenic double bonds, see Fig. 8a and b of Ref. [41]. Therefore one

can argue that the magnetotropism of heterocyclic pentatomics is characterized by a mix of two different mechanisms, one typical of systems with isolated, the other with conjugated, C–C bonds.

The plots of streamlines and modulus of the π current densities in C_4H_4X pentatomics with $C_{2v}(C_s)$ symmetry, on the plane at 1 bohr over that of the molecule, close to the region of maximum π charge density, confirm the presence of ring currents, see Figs. 4, 5, 6, 7. However, their intensity over the conjugated segment of four carbon atoms is smaller than that evaluated in benzene and in the cyclopentadienyl anion $C_5H_5^-$.

Figure 4 shows that, in the 1,3-cyclopentadiene molecule, the π electrons sustain ring currents to a smaller extent than in the other pentatomics. Localised circulations, embedded within the peripheral main stream, appear about the formal C–C double bonds. Figs. 8 and 9 show spiral flow typical of partially (or non) conjugated C–C bonds [41] also in phosphole and arsole.
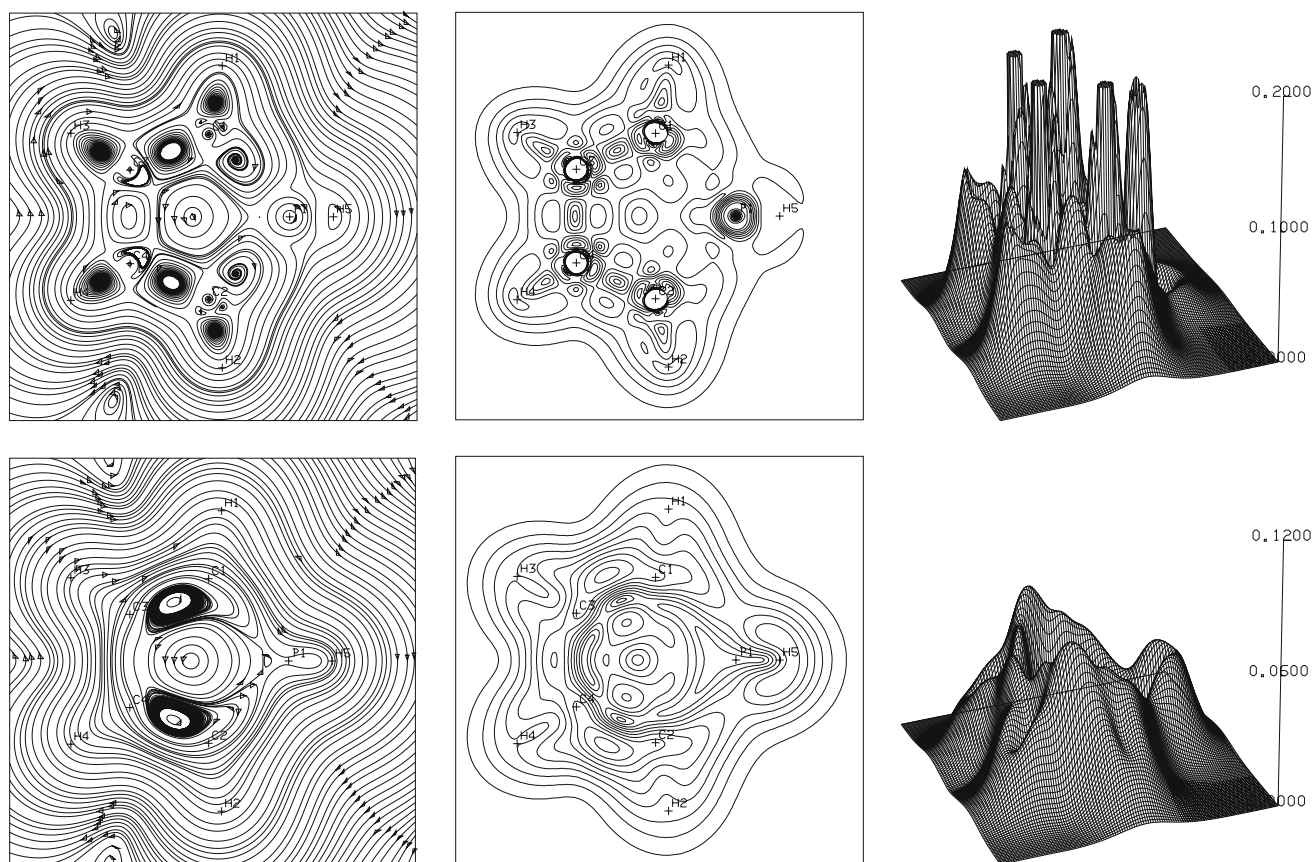
Fig. 8 Phosphole molecule. *Top* streamlines, contour map (in steps of 2×10^{-2} au up to the maximum value 1.80 au) and three-dimensional perspective view of the modulus |**J**| for the total induced current density on a plane passing through the centre of mass and parallel to four carbon atoms. *Bottom* streamlines, contour map (in steps of 7×10^{-3} au up to the maximum value 0.07 au) and three-dimensional perspective view of the total induced current density on a plane parallel to four carbon atoms, at 1.0 bohr above the centre of mass. The magnetic field (of magnitude 1 au) points perpendicularly outward the plot plane

4 Concluding remarks

A three-dimensional model has been obtained to describe the quantum mechanical electron current density field **J** induced in heterocyclic conjugated compounds C_4H_4X, with $X=CH_2$, NH, O, S, PH, and AsH, by an external magnetic field perpendicular to the plane of the four ring carbon atoms. A compact description of the current density vector field is provided by the Gomes stagnation graph defined by the singularities, i.e., isolated points and one-dimensional manifolds at which the modulus of **J** vanishes.

A marked difference has been observed between the stagnation graph of diatropic C_nH_n aromatic cyclic molecules and that of C_4H_4X heterocyclic ring compounds. The former is characterized by a cage of stagnation lines branching out of the primary diamagnetic vortex, which flows in the tail regions of the molecular domain, into n diamagnetic vortices ending up on the molecular plane.

The latter, for different X heteroatoms, contains a disconnected closed stagnation loop, passing close to the midpoint of the pentagon side opposite to X, and crossing the plane of the carbon atoms in the proximity of the centre of mass. Thus the central paramagnetic vortices observed in C_nH_n and C_4H_4X are sustained by different mechanisms and have different evolution in space.

The stagnation graphs of pentatomic planar molecules contain another common feature, i.e., an axial vortex flowing in the vicinity of the heteroatom and extending to the outer regions, where the corresponding stagnation line becomes approximately parallel to the external magnetic field. The models obtained help clarify significative differences between the magnetic response of C_nH_n and C_4H_4X molecules. The latter are characterised by a superimposition of the π diatropism typical of aromatic C_nH_n rings with spiral flow documented in allene systems. The plots show that 1,3-cyclopentadiene molecule actually sustains ring currents, but
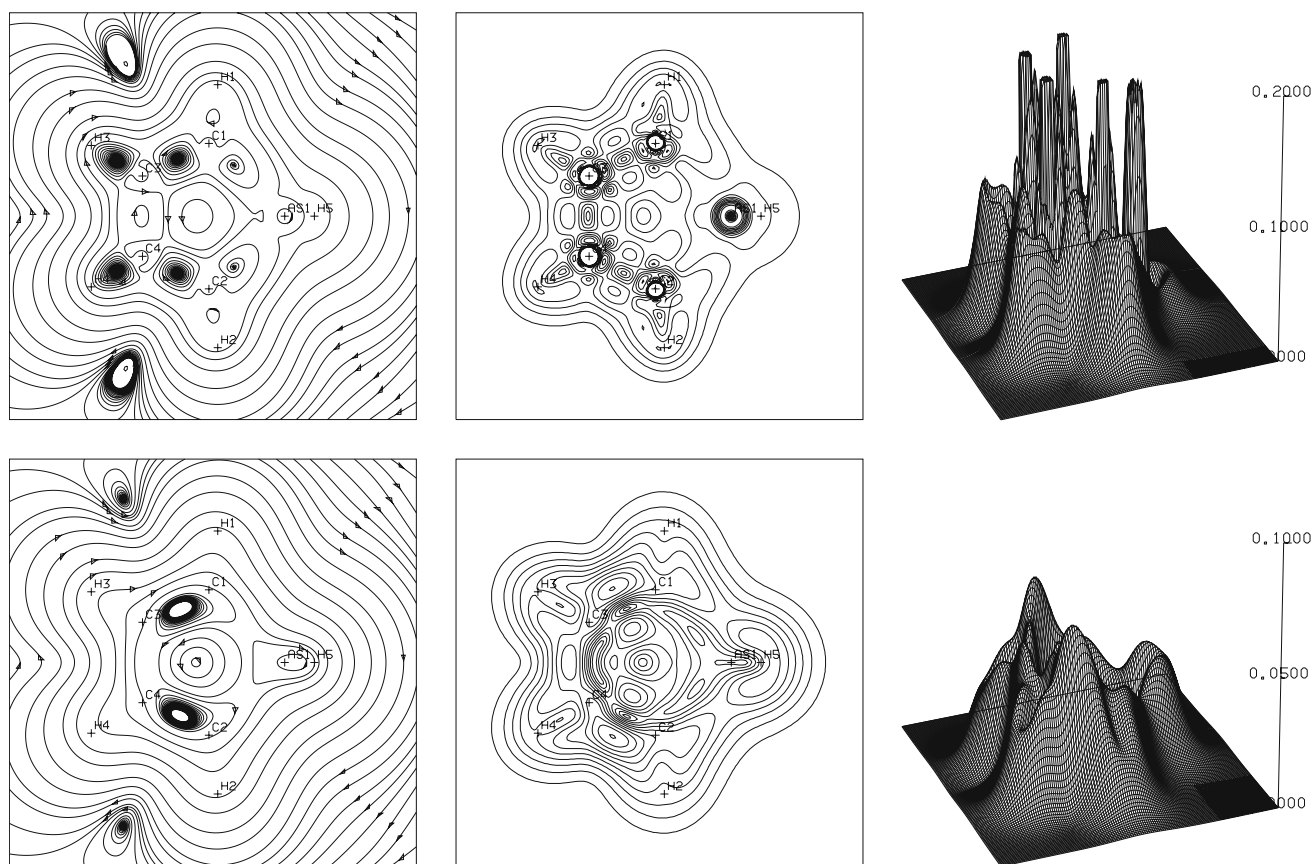
Fig. 9 Arsole molecule. *Top* streamlines, contour map (in steps of 2×10^{-2} au up to the maximum value $\approx$1.90 au) and three-dimensional perspective view of the modulus |**J**| (in au) for the total induced current density on a plane passing through the centre of mass and parallel to four carbon atoms. *Bottom* streamlines, contour map (in steps of 6×10^{-3} au up to the maximum value $\approx$0.07 au) and three-dimensional perspective view of the total induced current density on a plane parallel to four carbon atoms, at 1.0 bohr above the centre of mass. The magnetic field (of magnitude 1 au) points perpendicularly outward the plot plane

to a lesser extent than the heterocyclic pentatomics, and that the π electrons give rise to the typical spiral flow localised about non aromatic C = C bonds.

References

1. Bernstein HJ, Schneider WG, Pople JA (1956) Proc Roy Soc (London) A 236:515
2. Pople JA (1956) J Chem Phys 24:1111
3. McWeeny R (1958) Mol Phys 1:311
4. Pauling L (1936) J Chem Phys 4:673
5. Lonsdale K (1937) Proc Roy Soc (London) A 159:149
6. London F (1937) J Phys Radium 8:397, 7ème Série
7. London F (1937) C R Acad Sci (Paris) 205:28
8. London F (1937) J Chem Phys 5:837
9. Lazzeretti P (2000) Ring currents. In: Emsley JW, Feeney J, Sutcliffe LH (eds) Progress in nuclear magnetic resonance spectroscopy, vol. 36. Elsevier, pp 1–88
10. von Ragué Schleyer P (2001) Chem Rev 101:1115, and articles therein
11. Gomes JANF, Mallion RB (2001) Chem Rev 101:1349
12. Randić M (2003) Chem Rev 103:3449
13. von Ragué Schleyer P (2005) Chem Rev 105:3433, and articles therein
14. Lazzeretti P, Zanasi R (1981) Chem Phys Lett 80:533
15. Lazzeretti P, Zanasi R (1982) J Chem Phys 77:3129
16. Lazzeretti P, Rossi E, Zanasi R (1982) Nuovo Cimento 1D:70
17. Ligabue A, Soncini A, Lazzeretti P (2002) J Am Chem Soc 124:2008
18. Musher JI (1966) Theory of the chemical shift. In: Waugh JS (ed) Advances in magnetic resonance, vol. 2. Academic, New York, pp 177–224
19. Fleischer U, Kutzelnigg W, Lazzeretti P, Mühlenkamp V (1994) J Am Chem Soc 116:5298
20. Keith TA, Bader RFW (1993) Chem Phys Lett 210:223
21. Bader RFW, Keith TA (1993) J Chem Phys 99:3683
22. Gomes JANF (1983) J Chem Phys 78:4585
23. Gomes JANF (1983) Phys Rev A 28:559

24. Gomes JANF (1983) J Mol Struct (THEOCHEM) 93:111
25. Pelloni S, Faglioni F, Zanasi R, Lazzeretti P (2006) Phys Rev A 74:012506
26. Johansson MP, Jusélius J (2005) Lett Org Chem 2:469
27. Jameson CJ, Buckingham AD (1979) J Phys Chem 83:3366
28. Jameson CJ, Buckingham AD (1980) J Chem Phys 73:5684
29. Lazzeretti P, Zanasi R (1983) Chem Phys Lett 100:67
30. Ferraro MB, Lazzeretti P, Viglione RG, Zanasi R (2004) Chem Phys Lett 390:268
31. Soncini A, Fowler PW, Lazzeretti P, Zanasi R (2005) Chem Phys Lett 401:164
32. Pelloni S, Ligabue A, Lazzeretti P (2004) Org Lett 6:4451
33. Ferraro MB, Faglioni F, Ligabue A, Pelloni S, Lazzeretti P (2005) Magn Res Chem 43:316
34. von Ragué Schleyer P, Maerker C, Dransfeld A, Jiao H, van Eikema Hommes NJR (1996) J Am Chem Soc 118:6317
35. Cyrański M, Krygowski TM, Katrizky AR, von Ragué Schleyer P (2002) J Org Chem 67:1333
36. Wannere CS, Corminboeuf C, Allen WD, Schaefer HF III, von Ragué Schleyer P (2005) Org Lett 7:1457
37. Chesnut DB (1998) Chem Phys 231:1
38. Chesnut DB, Bartolotti LJ (2000) Chem Phys 253:1
39. Cyrański M, von Ragué Schleyer P, Krygowski TM, Jiao H, Hohlneicher G (2003) Tetrahedron 59:1637
40. Collard K, Hall GG (1977) Int J Quantum Chem XII:623
41. Keith TA, Bader RFW (1993) J Chem Phys 99:3669
42. If the eigenvalues are complex one defines the signature as the difference between the number of eigenvalues having a positive real part and the number of eigenvalues having a negative real part
43. Gomes JANF (1983) J Chem Phys 78:3133
44. Coddington EA, Levinson N (1955) Theory of ordinary differential equations. Mc Graw–Hill, New York
45. Hirschfelder JO (1977) J Chem Phys 67:5477
46. Hamermesh M (1972) Group theory and its applications to physical problems. Addison-Wesley, London
47. van Duijneveldt FB (1971) Gaussian basis sets for the atoms H-Ne for use in molecular calculations. Research Report RJ 945, IBM
48. Pelloni S, Faglioni F, Soncini A, Ligabue A, Lazzeretti P (2003) Chem Phys Lett 375:583
49. McLean AD, Chandler GS (1980) J Chem Phys 72:5639
50. Woon DE, Dunning TH, Jr (1993) J Chem Phys 98:1358
51. Frisch MJ et al (1998) Gaussian 98, Revision A.7. Gaussian, Inc., Pittsburgh
52. Lazzeretti P, Malagoli M, Zanasi R (1994) Chem Phys Lett 220:299
53. Lazzeretti P (2003) Electric, magnetic properties of molecules. In: Wilson S (ed) Handbook of molecular physics, quantum chemistry, Vol. 3, Part 1, Chap. 3. Wiley, Chichester, pp 53–145
54. Coriani S, Lazzeretti P, Malagoli M, Zanasi R (1994) Theor Chim Acta 89:181
55. Zanasi R (1996) J Chem Phys 105:1460
56. Soncini A, Lazzeretti P, Zanasi R (2006) Chem Phys Lett 421:21
57. Parker TS, Chua LO (1986) Practical numerical algorithms for chaotic systems. Springer, Berlin Heidelberg New York
58. The LINUX and WINDOWS versions of the graphic code used to obtain three-dimensional representations of the stagnation graph and current density vector field of a series of molecules can be downloaded at https://theochem.chimfar.unimo.it/STAGNATION-GRAPH/
59. Lazzeretti P (2004) Phys Chem Chem Phys 6:217